

Adsorption Kinetic and Isotherm Studies of Reactive Red B Textile Dye Removal Using Activated Coconut Leaf Stalk

I Ketut Sudiana^{1*}, I Dewa Ketut Sastrawidana¹, I Nyoman Sukarta¹

¹ Department of Chemistry, Faculty of Mathematics and Natural Sciences, Universitas Pendidikan Ganesha, Singaraja, 81116, Bali, Indonesia

* Corresponding author's e-mail: sudi.ana@undiksha.ac.id

ABSTRACT

Textile wastewater has become one of the serious environmental problems due to containing a high concentration of chemicals with extreme color intensity. Reactive red RB is among the synthetic azo dyes commonly used as a textile colorant with their property are very difficult to degrade naturally. This research was focused on studying the kinetic behavior, and adsorption isotherm of reactive red RB textile dye on coconut leaf stalk activated carbon (CLSC). Coconut leaf stalk carbon was activated using sulphuric acid and sodium hydroxide. It was investigated in terms of chemical functional groups, surface morphology, carbon content, ash content, and adsorption efficiency of reactive red RB textile dye under various conditions of initial pH, incubation time, and dye concentration. The results showed the maximum adsorption efficiency of reactive red RB dye with a concentration dye of 60 mg/l onto CLSC surface activated by sulfuric acid and sodium hydroxide in an experiment carried out at pH 5 for 120 min were 88.73% and 64.27%, respectively. The adsorption isotherm of reactive red RB on the CLSC surface follows the Langmuir isotherm model, which shows that the adsorption process occurs monolayer. In contrast, the adsorption kinetics correspond to pseudo-second-order.

Keywords: adsorption kinetic, Isotherm adsorption, reactive red B textile dye, coconut leaf stalk carbon.

INTRODUCTION

Discharging textile wastewater into the environment has stimulated problems for human health and aquatic living systems. The textile industry effluents are high in chemical oxygen demand (COD), biological oxygen demand (BOD), and suspended solids (SS) with extremely color intensity [Yaseen and Scholz, 2019]. The value color intensity, COD, BOD, and TSS of textile wastewater are in the range of 50–2500 Pt-Co, 150–12.00 mg/L, 80–6000 mg/L, and 15–8000 mg/L [Al-Kdasi et al., 2005; Upadhye and Joshi, 2012; Hussein, 2013; Ghalya et al., 2014]. Estimated that 10–15% of synthetic dyes used are released from the fabric during the dyeing process and discharged into the environment as wastewater [Hassaan and Nerm, 2017]. The presence of color in the water causes inhibition of light penetration into the water, thereby impairing the

photosynthesis process of aquatic plants. As a result, the limited availability of oxygen in the water triggers the activity of anaerobic microorganisms that produce products with unpleasant odors. According to EPA, 2014 for water quality and effluent standards, the permissible limit of color, BOD, COD, and SS for printing, dyeing, and finishing industry are 550 TCU, 30 mg/L, 160 mg/L, and 30 mg/L, respectively. In addition, as stated in Regulation of the Minister of Health of Indonesia Number 32 of 2017, the maximum acceptable level of color for water sanitation is 50 TCU.

Reactive red RB is one of the synthetic dyes commonly used as colorants in fabric dyeing, belonging to the anionic mono-azo dye group. Most of the reactive dyes interact with cotton and wool through covalent bonds. The release of reactive dyes from the fabric is caused by the low degree of fixation, so they are easily hydrolyzed into the aqueous phase [Bhattacharyya et

al., 2005]. It is necessary to treat textile wastewater before being discharged into the water bodies to prevent environmental problems, especially in aquatic ecosystems.

Numerous biological, chemical, and Physico-chemical methods have been successfully developed and implemented in textile wastewater treatment. Several biological methods which are applied such as using bacterial biofloculants isolated from activated sludge [Buthelezi et al., 2012; Mirbolooki et al., 2017], wood degrading fungi [Sudiana et al., 2022] and anaerob-aerob bacteria [Naimabadi, 2009]. The chemical methods applied such as advanced oxidation process [Patil and Rault, 2014; Buthiyappan et al., 2019; Ilhan et al., 2019], electrochemical oxidation [Latha et al., 2017; Sastrawidana et al., 2018], whereas the Physico-chemical method such as photocatalysis [Hussein and Abbas, 2010; Agustina et al., 2020; Sagadevan et al., 2022] and adsorption [Rahman and Akter, 2016; Firdaus et al., 2017; Patel, 2018; Sukarta et al., 2021]. Among these methods, adsorption has advantages, including low cost, high conversion efficiency, easy operation, not producing secondary pollutants, and being easily regenerated through the desorption process [Piaskowski et al., 2018; Ali et al., 2018]. Generally, separation by adsorption is based on the attraction of pollutants from the fluid phase to the adsorbent surface through physical or chemical bonds. Properties of the adsorbent surface involving the polarity, pore size, surface area, and operational conditions such as pH, contact time, and adsorbate concentration significantly affect the adsorption capacity [Tanthapanichakoo et al., 2005]. Different materials such zeolite/acanthophora spicifera nanoporous composite [Hamd et al., 2021], starch/polyvinyl alcohol composite [Xia et al., 2020], organoclay [Patanjali et al., 2021], activated carbon [Yusop et al., 2021], and agricultural wastes [Bhatti et al., 2015; Farhadi et al., 2021] have been used as adsorbents in textile wastewater treatment.

Among types of available adsorbents, activated carbon is a promising adsorbent for wastewater treatment due to its ease of obtaining and have a high adsorption capacity. Activated carbon can be prepared from rice husks, sawdust, bamboo, corn stalks, and other carbonaceous natural materials, including agricultural waste. Using activated carbon from agricultural waste for wastewater treatment has several advantages, including its availability in large quantities, low cost, and its

surface containing various functional groups that play an important role in the adsorption process [Farhadi et al., 2021]. Several functional groups such as carboxylic acid ($-\text{COOH}$), hydroxyl ($-\text{OH}$), carbonyl ($-\text{C}=\text{O}$), amine ($-\text{NH}_2$), and ester ($-\text{O}-$) groups are present in various agricultural wastes that are relevant to their adsorption characteristics. The activated carbon from agricultural waste have widely used for textile wastewater adsorption such as sugarcane bagasse [Liew Abdullah, et al., 2005], Rice husk ash [Oladoja, et al., 2008], peanut hull [Etoriki and Masoudi, 2011], orange peel powder [Munagapati and Dong-Su Kim, 2016], aloe vera leaves shell [Khaniabadi et al., 2017], psyllium stalks [Pariyaraman et al., 2019], and coffee waste [Block et al., 2021]. Adsorption behavior such as kinetic and isotherm adsorption of dyes onto carbon from agricultural waste has not been widely discussed in previous research. This study investigates the kinetic and thermodynamic adsorption properties of reactive RR-RB on activated and non-activated CLSC. The non-activated and activated CLSC characterized their properties, including moisture, volatile matter, ash content, and carbon content using thermogravimetric analysis. The microstructure surface is investigated under SEM observation and functional group analysis using FTIR. The color removal efficiency of batch adsorption was investigated in different operational conditions, such as the effect of initial pH, contact time, and dye concentration.

MATERIALS AND METHODS

Dye

Commercially reactive red RB produced by Sigma-Aldrich with CAS number 17095-24-8. The chemical structure of this dye is shown in Figure 1.

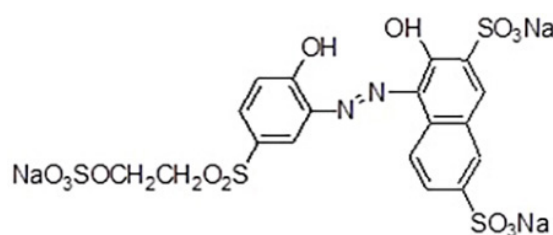


Figure 1. Chemical structure of the reactive red RB dye

Preparation of CLSC

The coconut leaf stalks obtained from a local coconut plant in Bali, Indonesia were cut into small pieces (less than 2×2 cm). The coconut leaf stalk was cleaned with aquades several times to remove dust and dirt. The carbon powder was prepared by heating the coconut leaf stalk in a vacuum furnace at 500 °C for 30 min. The carbon was crushed using a grinder machine and then converted to a fine powder with a ball milling machine for 24 h. The metal oxides contained in the fine carbon powder were separated by dissolving them in 0.5 M HCl solution for 24 hours, then neutralized with NaOH solution, and finally dried in an oven at 105 °C until a constant weight was obtained. The carbon powder was sieved with a sieve size of 200 mesh.

Activation of CLSC

The CLSC were separately immersed in a 0.3 M sodium hydroxide and 0.3 M sulfuric acid solution at room temperature for 24 hours while continuously shaking. Each CLSC sample was washed repeatedly with water until a neutral pH was obtained, then dried at 105 °C for 24 h to prepare activated CLSC. Activated CLSCs were characterized and tested for their ability to degrade reactive red textile dye RB through the batch technique.

Characterization of CLSC

Activated and non-activated CLSCs were analyzed for their moisture, volatile matter, ash, and carbon content using a Thermogravimetric analyzer (TGA). Functional groups of CLSC were identified using Fourier Transform Infrared (FTIR), while the surface morphology was observed under scanning electron microscopy (SEM) with 10000 x magnifications. The characteristics of activated and unactivated CLSC from the TGA thermogram are presented in Table 1.

Batch adsorption studies

The adsorption experiments of reactive red RB dye on activated and non-activated CLSC were separately carried out using a batch technique. A total mass of 0.20 g of CLSC was added to 100 mL of a 50 mg/L dye solution placed in a glass vial covered with aluminum foil, and then the mixture was aged for 160 min. while being shaken at 150 rpm using an automatic shaker. The mixture was filtered with Whatman filter paper No.1 and their filtrate was centrifuged at 3000 rpm using a thermo-scientific centrifuge. The adsorption capacity of dye on CLSC surface was determined by measuring absorbance before and after treatment using a UV-Vis spectrophotometer at 519 nm. Several operational parameters, including the effect of initial pH (3–10), dyestuff concentration (10–80 mg/L), and contact time (20–180 min.), were investigated to find out the optimum conditions and adsorption behavior of dye on CLSC surfaces. The adsorption efficiency of dye on CLSC surface is calculated using equation 1.

$$\text{Adsorption efficiency (\%)} = \frac{C_o - C_i}{C_o} \times 100\% \quad (1)$$

where: C_o and C_i are the initial and final absorbance of remazol red RB dye solution (mg/L).

Adsorption isotherm studies

The adsorption isotherm is used to describe the adsorbate-adsorbent interaction. This study used Langmuir and Freundlich's isotherm to describe equilibrium adsorption. Langmuir assumes that the adsorption of adsorbate occurs on a homogeneous adsorbent surface. The Langmuir equation is defined as:

$$\frac{1}{qe} = \frac{1}{qm} + \frac{1}{k qm Ce} \quad (2)$$

where: qe is amount of adsorbate on adsorbent at equilibrium state (mg/g);

Table 1. Characteristics of CLSC

Properties	Non-activated CLSC	Activated CLSC	
		Activated with H ₂ SO ₄	Activated with NaOH
Moisture (% w/w)	13.83	10.74	14.00
Volatile (% w/w)	30.40	33.03	31.84
Ash content (% w/w)	9.17	8.71	10.77
Fixed carbon (% w/w)	43.39	47.51	46.59

q_{max} is the maximum of adsorption capacity (mg/g), k is the equilibrium constant of Langmuir adsorption (L/mg); C_e is the adsorbate equilibrium concentration (mg/L).

The plot of $1/q_e$ vs. $1/C_e$ and then the k and q_{max} values were calculated from slope and intercept of curve, respectively.

The Freundlich of adsorption models assumes that multilayer adsorption occurs on heterogeneous adsorbent surfaces. The empirical of Freundlich isotherm equation is written as

$$\ln q_e = \ln k + \frac{1}{n} \ln C_e \quad (3)$$

where: q_e is the amount of reactive red RB in the adsorbent at equilibrium (mg/g).

Kinetic studies

The kinetics of reactive red RB dye by activated and non-activated of CLSC were studied through two common models; pseudo-first order and pseudo-second order models. The pseudo-first order is generally expressed by equation:

$$\ln(q_e - q_t) = \ln q_e - k_1 t \quad (4)$$

While, the pseudo-second order model is represented by equation

$$\frac{t}{q_t} = \frac{1}{k_2 q_e^2} + \frac{1}{q_e} t \quad (5)$$

where: q_e and q_t are the amount of reactive red RB adsorbed by CLSC at equilibrium and at time t (mg/g), respectively. The constant of pseudo-first order (min^{-1}) and pseudo-second order (mg/g.min) were represented as k_1 and k_2 , respectively.

RESULTS AND DISCUSSIONS

FTIR Spectra of CLSC

Some characteristics of functional groups of CLSC were identified by Fourier transform infrared (FTIR) spectroscopy at the spectra range of 4000 to 500 cm^{-1} with 10000 x magnifications. The FTIR spectra of the CLSC samples before and after being activated with H_2SO_4 and NaOH are shown in Figure 2.

It was clearly observed in Figure 2 that the FTIR spectrum of acid-activated CLSC, alkaline-activated CLSC, and non-activated CLSC showed similar peaks with slight changes in relative intensity. All spectra show a wide broad band in the range of 3032–3406 cm^{-1} is assigned to O-H stretching vibration [Zhang et al., 2018]. The absorption peak around 1580 cm^{-1} corresponds to carboxyl-carbonate structures or to aromatic C=C [Moreno-Castilla et al., 2000]. The peaks in the region from 800 cm^{-1} to 1200 cm^{-1} indicate to C-C stretching [Wibawa et al., 2020]

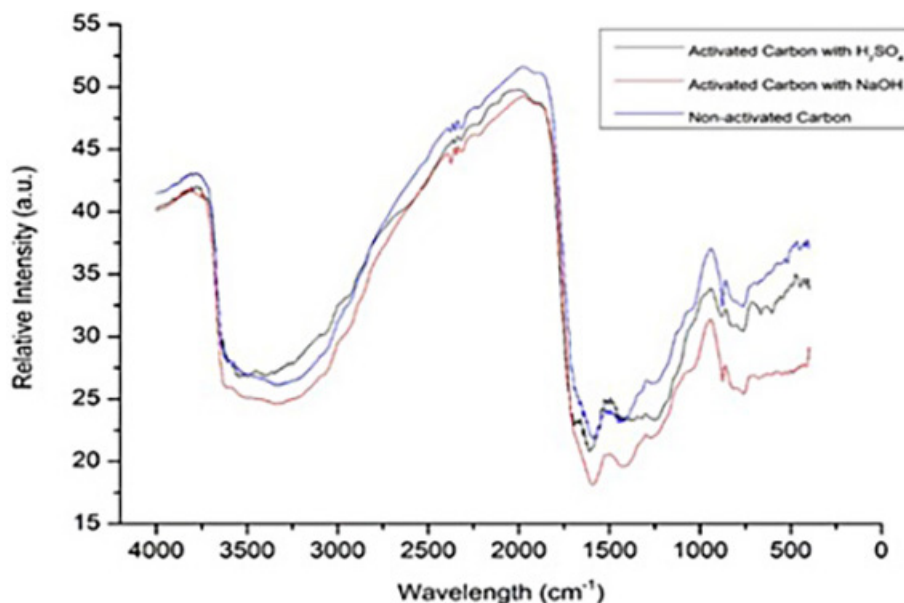


Figure 2. FTIR spectra of CLSC (a) without activation, (b) activation with H_2SO_4 , and (c) activation with NaOH

Surface morphology

SEM analyzes the surface morphology of the non-activated carbon and activated carbon with sulphuric acid and sodium hydroxide; the images are shown in Figure 3. According to Figure 3, the surface features of the three CLSCs are rough and irregular, along with heterogeneous cavities distributed on the CLSC surface. However, the cavities and pore size distribution of CLSC sample activated by H_2SO_4 is higher than CLSC sample activated by NaOH and non-activated. Thus, CLSC activated using H_2SO_4 was a good adsorbent to absorb dye molecules from the aqueous phase.

Adsorption studies

Effect of initial pH on adsorption efficiency of dye

The pH of the dye solution is one of the important factors that significantly affect the adsorption ability of the dye on the CLSC surface. The pH of a medium will control the magnitude of electrostatic charges, which are imparted by the ionized dye molecules. Generally, at a low pH solution, the adsorption efficiency will increase for

anionic dye adsorption and decrease for cationic dye adsorption (Saleh et al., 2011). The effect of the initial pH medium on the adsorption efficiency of reactive red RB onto CLSC is shown in Figure 4.

Figure 4 shows that the efficiency of dye adsorption onto activated and unactivated CLSCs was significantly affected by the pH of the medium. The color removal efficiency of reactive red RB increased with increasing the pH medium from 3 to 5 for all adsorbents, then gradually decreased to pH 10. In this study, CLSC activated with H_2SO_4 has a higher adsorption capacity than CLSC activated with NaOH and without activation. The maximum removal of reactive red RB was observed at pH 5. The adsorption efficiency of dye on CLSC non-activated, activated with H_2SO_4 and NaOH were 23.37%, 62.11% and 26.72%, respectively. This finding is in line with Ali et al., 2020. This finding is in line with Abi et al., 2020, which found the optimum pH for anionic acid blue dye adsorption using activated charcoal was pH 5. They argued that at low pH, the surface of the activated charcoal becomes more positively charged, caused by the increase of hydrogen ion concentration, thereby enhancing

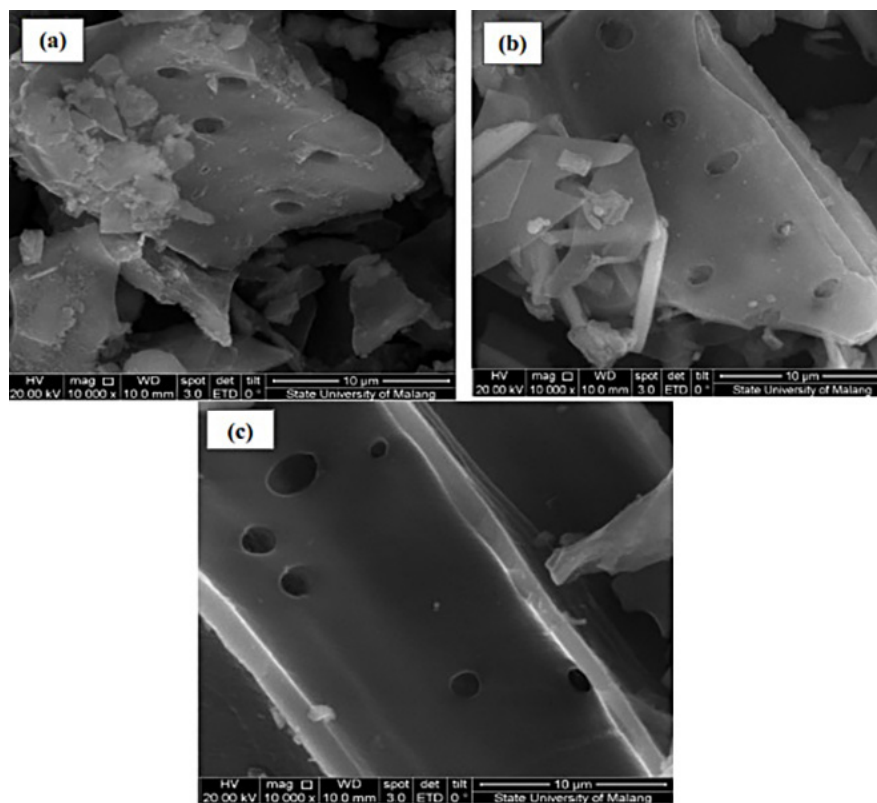


Figure 3. SEM images of CLSC at 10000x magnifications (a) non-activated CLSC, (b) activated CLSC with H_2SO_4 and (c) activated CLSC with NaOH

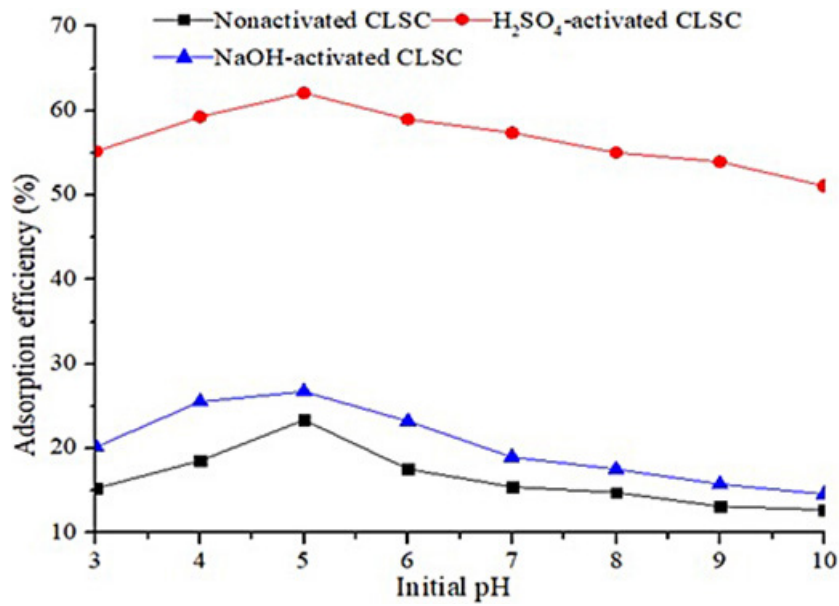
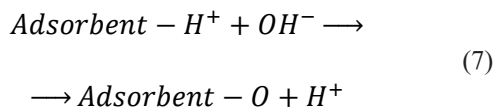
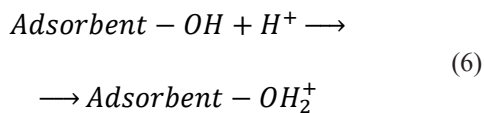


Figure 4. Adsorption efficiency of reactive red RB onto CLSC at different initial pH medium

the adsorption of the negatively charged acid blue dye. The effect of pH on adsorbent surface charge has been proposed by Ko et al., 2003.



At low pH, the surface of CLSC is positively charged due to protonation action, so it is more favorable for the absorption of anion species. Whereas, at higher pH media, the surface

of CLSC has a negative charge which favors the adsorption of cations. In addition, reactive red RB is an anionic monoazo dye which more easily adsorbed at a lower pH due to an increase in the electrostatic interaction between negatively charged reactive red RB and positively charged CLSC surface (Pathania et al., 2017).

Effect of contact time on adsorption efficiency of dye

The adsorption efficiency of non-activated and activated CLSC for reactive red RB textile dye was studied over a contact time range of 20–200 min. as presented in Figure 5. In general, the dye removal efficiency increases with an

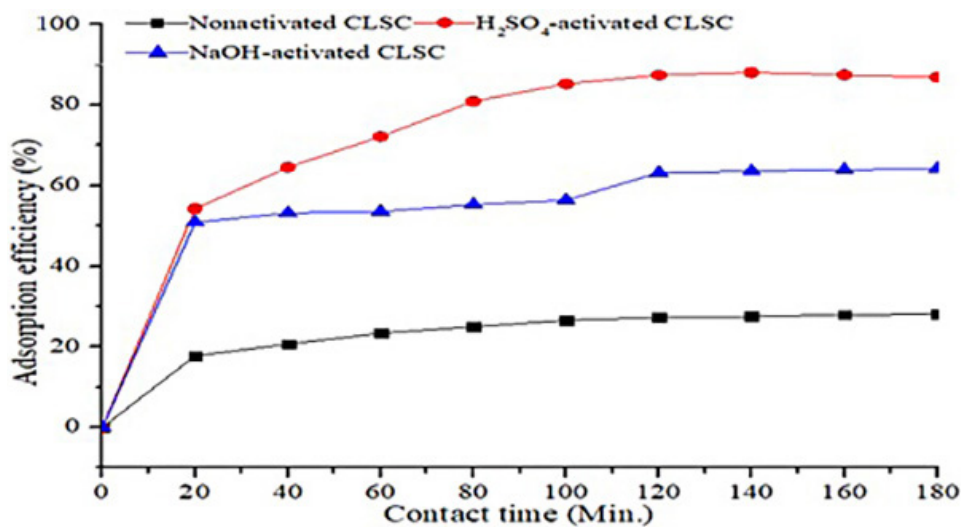


Figure 5. Adsorption efficiency of reactive red RB onto CLSC at different contact time

extended contact time. As shown in Fig. 5, the removal rate was rapidly increased in the first 15 min. and then steadily to achieve equilibrium adsorption within 120 min. The maximum adsorption efficiency was observed at 73.25% at 120 min. of contact time.

As can be seen from Figure 5, reactive red RB adsorption onto CLSC occurred in two steps. In the first step, fast reactive red RB adsorption occurred in 15 min due to many available cavities and active sites on the adsorbents. In the second step, the adsorption process occurs until the active site or cavity of CLSC becomes saturated, and equilibrium is reached for CLSC at 120 min.

Effect of initial dye concentration on adsorption efficiency of dye

The adsorption efficiency of dye onto the adsorbent surface is highly dependent on the initial concentration of the dye. It is related to the availability of binding sites on the adsorbent. The effect of dye concentration on adsorption efficiency of reactive red RB onto CLSC is shown in Figure 6.

Figure 6 shows that adsorption efficiency increases as the initial dye concentration increase to 60 mg/L, and adsorption decreases with the increased dye concentration. This phenomenon can be described by the saturation of adsorption sites on the CLSC surface. In this case, the high mass transfer driving force at a high initial dye concentration then decreased with increasing saturation of the adsorbent site (Rapo and Tonk., 2021). The proportional initial dye concentration can act as a push for the adsorption process, support the

diffusion process, and mass transfer from the solution to the adsorbent surface. However, at higher dye concentrations, the availability of binding sites required to adsorb dye molecules is less. In our study, it was found that the optimum concentration of reactive red RB adsorbed by CLSC without activation, H_2SO_4 -activated CLSC, and NaOH-activated CLSC was 60 mg/L on the experiment conditioned at pH 5 and a contact time of 120 min., with the adsorption efficiency of 28.15%, 88.73%, and 64.27%, respectively. This result agrees with Rida et al., 2020 who state that when the number of available adsorption sites is high, more dyes can be absorbed. However, after a time when the number of available sites is reduced, the dye molecule takes longer to reach the least accessible site.

Adsorption kinetics modeling

The adsorption rate is an important factor for a better selection of materials to be used as an adsorbent. A good adsorbent should have a high adsorption capacity with a fast adsorption rate. In this study, the adsorption kinetic models of the reactive red RB textile dye on the nonactivated-CLSC, H_2SO_4 -activated CLSC and NaOH-activated CLSC were examined using pseudo-first-order and pseudo-second-order. The best-fit model can be chosen based on the linearity of the regression correlation coefficient (R^2). Experiment curve of adsorption kinetic model for the reactive red RB textile dye on the CLSC surface were shown in Figures 7 and 8

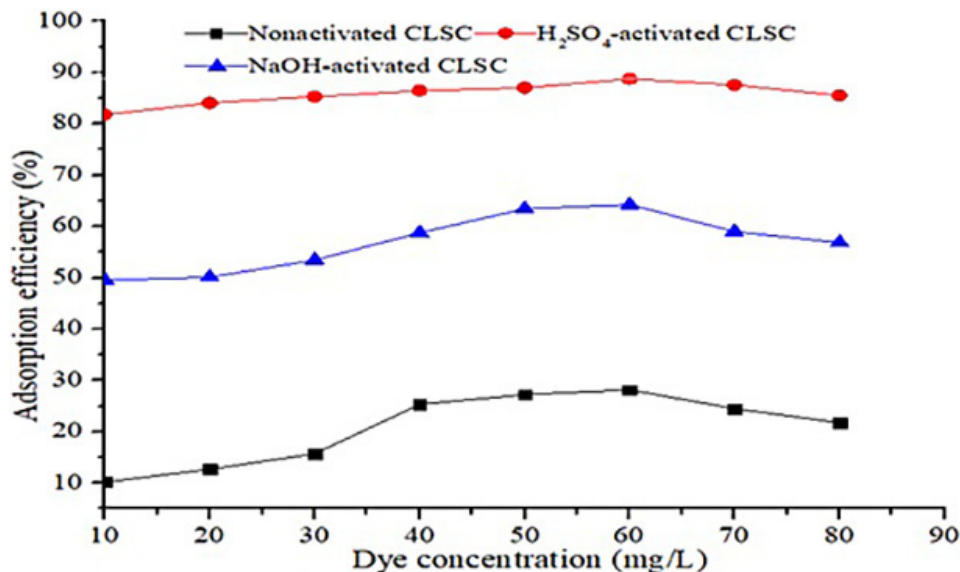


Figure 6. Adsorption efficiency of reactive red RB onto CLSC at different dye concentrations

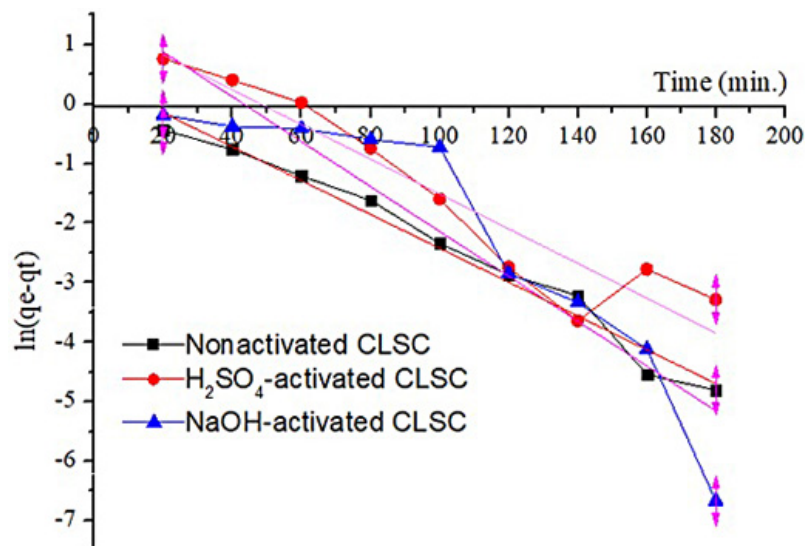


Figure 7. Adsorption kinetic models of pseudo-first-order for reactive red RB onto CLSC surface

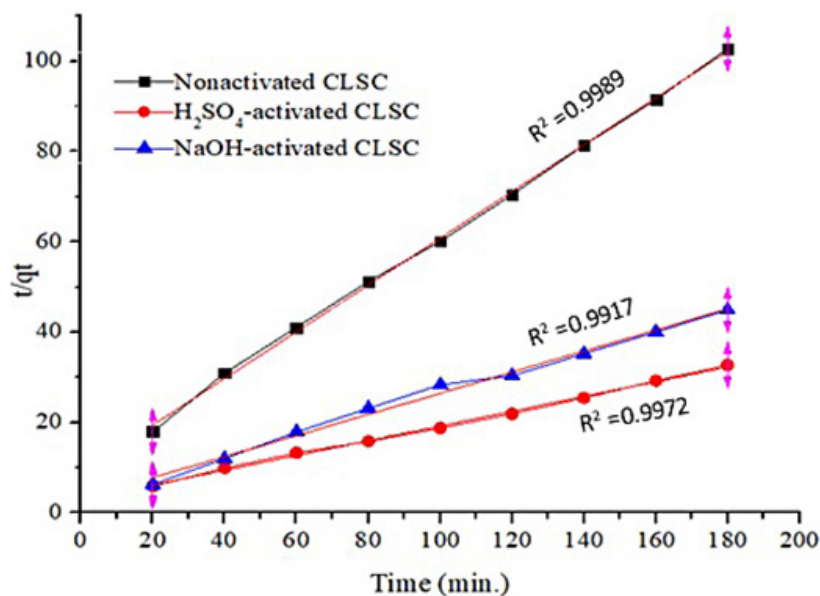


Figure 8. Adsorption kinetic models of pseudo-second-order for reactive red RB onto CLSC

Adsorption isotherms

The adsorption isotherm represents the relationship between the amounts of adsorbate adsorbed on the adsorbent surface at a constant temperature. The adsorption isotherm was evaluated using Langmuir and Freundlich isotherm models. A fitting adsorption isotherm model was conducted by comparing Langmuir and Freundlich isotherms' correlation coefficient (R^2). The adsorption isotherms were obtained at initial dye concentrations 10–80 mg/L range. The curve of Freundlich and Langmuir adsorption isotherms of reactive red RB onto CLSC are shown in Figures 9 and 10.

Figures 9 and 10 show the value of R^2 obtained from Langmuir and Freundlich isotherm were 0.9786 and 0.9354 for non-activated CLSC, CLSC activated with H_2SO_4 were 0.9847 and 0.9559 as well as 0.9782 and 0.9172 for CLSC activated with NaOH. The correlation coefficient value of Freundlich is lower than Langmuir value. Therefore, the reactive red RB textile dye favored monolayer adsorption by CLSC and corresponded to the Langmuir model. This finding is in line with Chaiwon and Chan- nei (2017). They reported that the adsorption of methyl orange dye on the carbon surface from bagasse activated by H_2SO_4 and NaOH fits the Langmuir adsorption isotherm model.

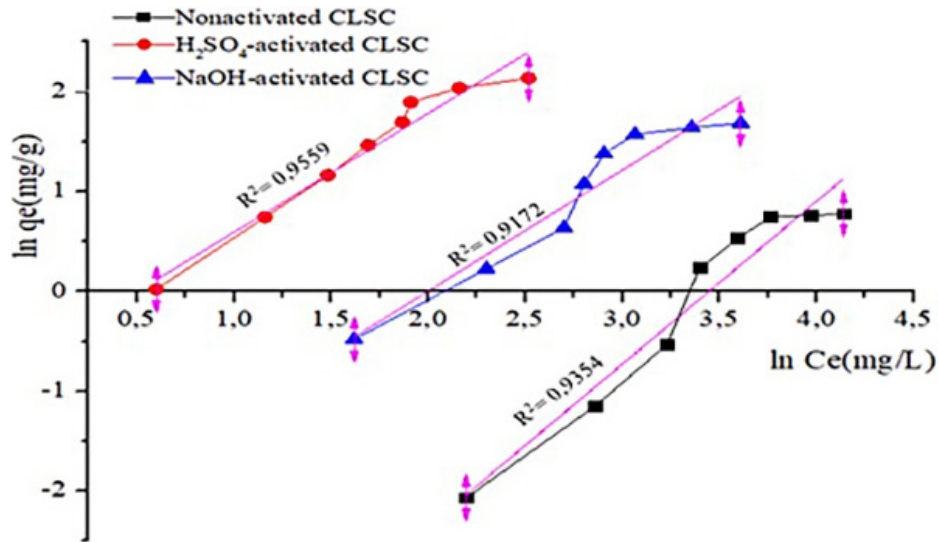


Figure 9. Langmuir adsorption isotherm curve of reactive red RB dye onto CLSC surface

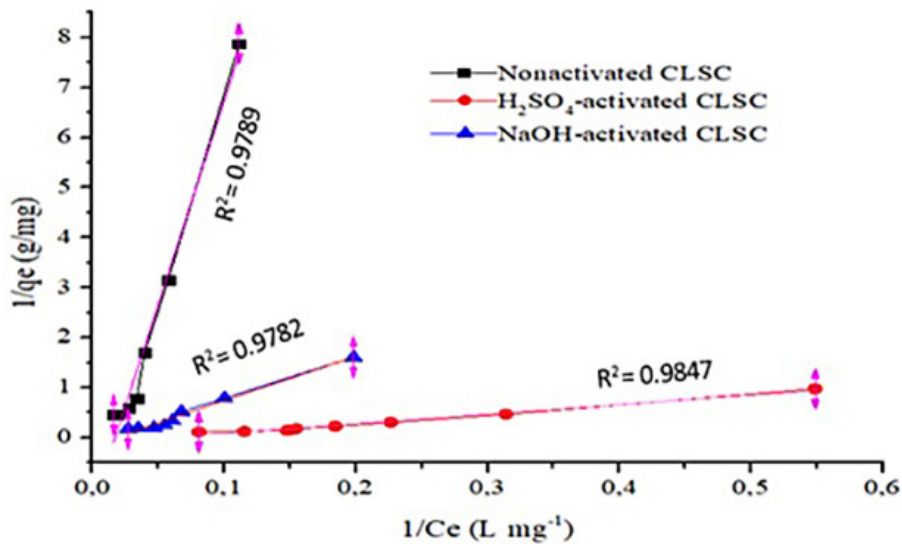


Figure 10. Freundlich adsorption isotherm curve of reactive red RB dye onto CLSC surface

CONCLUSIONS

In this study, CLSC activated with H_2SO_4 showed a higher adsorption capacity than CLSC activated with NaOH and without activation. Therefore, CLSC activated with H_2SO_4 is promising to be developed for removing reactive red RB textile dye. The maximum adsorption efficiency of reactive red RB dye by CLSC activated with H_2SO_4 was obtained at 88.73% at optimum operating parameters, including initial pH, dye concentration, and contact time were 5, 60 mg/L and 120 min. The adsorption isotherm was fitted well in the Langmuir isotherm models, confirming that the sorption is homogenous and occurred in physical interactions. The rate of sorption was found to obey pseudo-second-order kinetics.

Acknowledgments

The authors would like to thank the Chemistry Department, Faculty of Mathematics and Natural Sciences, Universitas Pendidikan Ganesha for providing the research facilities on data collecting services.

REFERENCES

1. Ali F., Ali N., Bibi I., Said A., Nawaz S., Ali Z., Salman S.M., Iqbal H.M.N., Bilal M. 2020. Adsorption isotherm, kinetics and thermodynamic of acid blue and basic blue dyes onto activated charcoal. *Case Studies in Chemical and Environmental Engineering*, 2, 1–6.
2. Ali N., Awais., Kamal T., Ul-Islam M., Khan A., Shah S.J., Zada A. 2018. Chitosan-coated cotton

- cloth supported copper nanoparticles for toxic dye reduction. *Int. J. Biol. Macromol.*, 111, 832–838.
3. Al-Kdasi A., Idris A., Saed K., Guan C.T. 2004. Treatment of textile wastewater by advanced oxidation processes - a review. *Global Nest Int. J.*, 6(3), 222–230.
 4. Agustina T.E., Melwita E., Bahrin D., Gayatri R., Purwaningtyas I.F. 2020. Synthesis of nano-photocatalyst ZnO-Natural Zeolite to degrade procion red. *Int. J. Technol.*, 11(3), 472–281.
 5. Bhatti H.N., Sadaf S., Aleem A. 2015. Treatment of textile effluents by low cost agricultural waste: Batch biosorption study. *J. Anim. Plant. Sci.*, 25(1), 284–289.
 6. Buthiyappan A., Azis A., Rahman A. 2019. Energy intensified integrated advanced oxidation technology for the treatment of recalcitrant industrial wastewater. *J. Clean. Prod.*, 206(1), 1025–1040.
 7. Buthelezi S.P., Ademola O., Olaniran, Pillay B. 2012. Textile dye removal from wastewater effluents using biofloculants produced by indigenous bacterial isolates. *Molecules*, 17, 14260–14274.
 8. Farhadi A., Ameri A., Tamjidi S. 2021. Application of agricultural wastes as a low-cost adsorbent for removal of heavy metals and dyes from wastewater: a review study. *Phys. Chem. Res.*, 9(2), 211–226.
 9. Firdaus M.L., Krisnanto N., Alwi W., Muhammad R., Serunting M.A. 2017. Adsorption of textile dye by activated carbon made from rice straw and oil palm midrib. *Aceh Int. J.Sci.Technol.*, 6(1), 1–7.
 10. Ghaly A.E., Ananthashankar R., Alhattab M., Ramakrishnan V.V. 2014. Production, characterization and treatment of textile effluents: a critical review. *J Chem. Eng. Process. Technol.*, 5(1), 1–18.
 11. Hamd A., Dryaz A.R., Shaban M., AlMohamadi H., Khulood A., Al-Ola A., Soliman N.K., Ahmed S.A. 2021. Fabrication and Application of zeolite/acanthophora spicifera nanoporous composite for adsorption of congo red dye from wastewater. *Nanomaterials*, 11(2441), 1–20.
 12. Hassaan M.A., Nembr A.E. 2017. Health and environmental impacts of dyes: Mini review. *Am. J. Environ. Sci. Eng.*, 1(3), 64–67.
 13. Hussein F.H. 2013. Chemical properties of treated textile dyeing wastewater. *Asian. J. Chem.*, 25(16), 9393–9400.
 14. Hussein, F., Abass, T. 2010. Solar Photocatalysis and Photocatalytic Treatment of Textile Industrial Wastewater. *Int. J. Chem. Sci.*, 8, 1409–1420.
 15. Ilhan F., Ulucan-Altuntas K., Dogan C., Kurt U. 2019. Treatability of raw textile wastewater using Fenton process and its comparison with chemical coagulation. *Desalin. Water. Treat.* 162, 142–148.
 16. Ko D.C.K., Tsang D.H.K., Porter F.J., McKay G. 2003. Applications of multipore model for mechanism identification during the adsorption of dye on activated carbon and bagasse pith. *Langmuir*, 19(3), 722–730.
 17. Latha A., Partheeban P., Ganesan R. 2017. Treatment of textile wastewater by electrochemical method. *Int. J. Earth Sci.*, 10(01), 146–149.
 18. Mirbooloki H., Amirnezhad R., Pendashteh A.R. 2017. Treatment of high saline textile wastewater by activated sludge microorganisms. *J. Appl. Res. Technol.*, 15(2), 167–172.
 19. Moreno-Castilla C., Lopez-Ramon M.V., Carrasco-Marín F. 2000. Changes in surface chemistry of activated carbons by wet oxidation. *Carbon*, 38, 1995–2001.
 20. Naimabadi A., Attar H.H., Shahsavani A. 2009. Decolorization and biological degradation of azo dye reactive Red 2 by anaerobic/aerobic sequential process. *Iran. J. Environ. Health. Sci. Eng.*, 6(2), 67–72.
 21. Patanjali P., Chopra I., Mandal A., Singh R. 2021. Kinetics and isotherm studies for adsorptive removal of methylene blue from aqueous solutions using organoclay. *Indian J. Chem. Technol.*, 28, 88–93.
 22. Pathania D., Sharma S., Singh P. 2017. Removal of methylene blue by adsorption onto activated carbon developed from *Ficus carica* bast. *Arabian J. Chem.*, 10, 1445–1450.
 23. Patil A. D., Raut P. D. 2014. Treatment of textile wastewater by Fenton's process as a advanced oxidation process. *J. Environ. Sci. Toxicol. Food. Technol.*, 8 (10), 29–32.
 24. Patel H. 2018. Charcoal as an adsorbent for textile wastewater treatment. *Sep. Sci.Technol.*, 53(17), 2797–2812.
 25. Piaskowski K., Swiderska-Dabrowska R., Zarzycki K. 2018. Dye removal from water and wastewater using various physical, chemical, and biological processes. *J. AOAC Int.*, 101(5), 1371–1384.
 26. Rahman F.B.A., Akter M. 2016. Removal of dyes from textile wastewater by adsorption using shrimp shell. *Int. J. Waste Resour.*, 6(3), 1–5.
 27. Rapo E., Tonk S. 2021. Factors Affecting Synthetic Dye Adsorption; Desorption Studies: A Review of Results from the Last Five Years (2017–2021). *Molecules*, 26(5419), 1–31.
 28. Rida K., Chaibeddra K., Cheraitia K. 2020. Adsorption of cationic dye methyl green from aqueous solution onto activated carbon prepared from *Brachychiton Populneus* fruit shell. *Indian J. Chem. Technol.* 27, 51–59.
 29. Sagadevan S., Fatimah I., Egbosiuba T. C., Alshahateet S. F., Lett J. A., Weldegebrerial G. K., Le M., Johan M. R. 2022. Photocatalytic efficiency of titanium dioxide for dyes and heavy metals removal from wastewater. *Bull. Chem. React.*, 17(2), 430–450.

30. Saleh M.A.M., Mahmoud D.K., Karim W.A.W.A., Idris A. 2011. Cationic and anionic dye adsorption by agricultural solid wastes: a comprehensive review. *Desalination*, 280, 1–13.
31. Sastrawidana D.K., Rachmawati D.O., Sudiana K. 2018. Color removal of textile wastewater using indirect electrochemical oxidation with multi carbon electrodes. *Environment Asia.*, 11(3), 170–181.
32. Sudiana I.K., Citrawathi D.M., Sastrawidana, I.D.K., Maryam S., Sukarta I.N., Wirawan G.A.H. 2022. Biodegradation of turquoise blue textile dye by wood degrading local fungi isolated from a plantation area. *J. Ecol. Eng.*, 23(7), 205–214.
33. Sukarta I.N., Ayuni N.P.S., Sastrawidana I.D.K. 2021. Utilization of khamir (*Saccharomyces cerevisiae*) as adsorbent of remazol red RB textile dyes. *Ecol. Eng. Environ. Technol.*, 22(1), 117–123.
34. Tanthapanichakoon W., Ariyadejwanich P., Japthong P., Nakagawa K., Mukai S. R., Tamon H. 2005. Adsorption–desorption characteristics of phenol and reactive dyes from aqueous solution on mesoporous activated carbon prepared from waste tires. *Water. Res.*, 39, 1347–1353.
35. Upadhye V. B., Joshi S.S. 2012. Advances in wastewater treatment: a review. *Int J Chem Sci Appl.*, 3(2), 264–268.
36. Wibawa P.J., Nur M., Asy'ari M., Nur H. 2020. SEM, XRD and FTIR analyses of both ultrasonic and heat generated activated carbon black microstructures. *Heliyon*, 6, e03546.
37. Xia K., Liu X., Wang W., Yang X., Zhang X. 2020. Synthesis of modified starch/polyvinyl alcohol composite for treating textile wastewater. *Polymers*, 12(289), 1–13.
38. Yaseen D. A., Scholz M. 2019. Textile dye wastewater characteristics and constituents of synthetic effluents: a critical review. *Int. J. Environ. Sci. Technol.*, 16, 1193–1226.
39. Yusop M.F.M., Ahmad M.A., Rosli N.A., Manaf M.E.A. 2021. Adsorption of cationic methylene blue dye using microwave-assisted activated carbon derived from acacia wood: Optimization and batch studies. *Arab. J. Chem.*, 14, 1–17.
40. Zhang L., Tu L., Liang Y., Chen Q., Li Z., Li C., Wang Z., Li W. 2018. Coconut-based activated carbon fibers for efficient adsorption of various organic dyes. *RSC Adv.*, 8, 42280–42291.